Monitoring of remedial works performance on landslide-affected areas through ground- and satellite-based techniques

Pierluigi Confuorto, Diego Di Martire, Donato Infante, Alessandro Novellino, Raffaele Papa, Domenico Calcaterra and Massimo Ramondini

Abstract

Differential Interferometric Synthetic Aperture Radar (DInSAR) techniques have been repeatedly proved as an effective tool for monitoring built environments affected by geological hazards. In this paper, it is described how the Coherent Pixel Technique (CPT) approach has been successfully applied to assess the response of an unstable slope to the different phases of remedial works following a landslide event. The CPT technique was performed on 59 COSMO-SkyMed images (May 2011 – August 2016) centered on the Quercianella settlement (a small hamlet of Livorno municipality, Tuscany, Italy), where the reactivation of a dormant shallow slide had occurred in March 2011 and, hereafter, a geotechnical intervention, designed with the aim of mitigating the risks, has been conducted from August 2013 lasting thirteen months. The time series of CPT results show a deformation pattern characterized by sudden accelerations (up to 21 mm in few months) in correspondence of the beginning of the interventions, during which the area has been excavated to install a drainage well, followed by mild decelerations and resulting from the stabilization of the area after the conclusion of the works. In particular, the integration of ground-based subsurface monitoring (inclinometers and piezometers) and DInSAR superficial data have provided consistent results for landslide characterization and helped in defining the state of activity and the areal distribution of the sliding surface. Moreover, the performance of remedial works installed in the landslide-affected area has been observed, showing the stabilization in the upper part of the hamlet and the still ongoing movement in the lower part. The combined monitoring system led

24 also the geotechnical company in charge to design further stabilization works as to preserve build-

25 ings and roads in the still moving area. Therefore, the integration of remote sensing techniques

26 and in situ instruments represents a timely and cost-efficient solution for monitoring intervention

27 works, opening new perspectives to engineering design for the stabilization of unstable slopes.

28 **Keywords:** DInSAR; COSMO-SkyMed; landslide; monitoring; remedial works; stability analy-

29 sis; landslide risk reduction.

1. Introduction

31   Landslides occur in several regions of the Earth, however, in Italy, one of the countries most affected,

32 16 victims and more than 2100 evacuees were reported in the 2017 only (IRPI, 2018). Landslides repre-

33 sent also a huge economic cost for the government: 4.47 billion euros have been invested by the Italian

34 Ministry of the Environment and other 44 billion euros would be necessary in policies and activities to

35 reduce areas vulnerable to hydrological or geological hazards (Salvati et al., 2010). Economic losses

36 related to natural risks have increased considerably in Europe and are expected to increase even more in

37 the future (EWCII, ONU, ISDR, 2003; United Nations, 2010; Mendelsohn and Saher, 2011; Vranken et

38 al., 2013). Direct damage includes physical impacts which lead to the destruction or to the reduction of

39 the functionality of an element (damage to property or facility) as well as to risk of killing or hurting

40 people. Therefore, costs of replacement, repair, or maintenance due to damage of property or facilities

41 within a landslide can all be considered as direct costs. Indirect damage includes reduced real estate

42 values, loss of productivity, lost revenue and loss of opportunity through the disruption of public services

43 and interruption of business continuity, and cost of measures to prevent or mitigate future mass move-

44 ment damage (Schuster and Fleming, 1986; Middelmann, 2007; Petrucci and Gullà, 2010; Vranken et

45 al., 2013).

46   Several landslides in the last century have been caused by human negligence and carelessness (e.g.

47 Guadagno et al. 1999; Sammarco, 2004; Bozzano et al., 2011; Notti et al., 2015) when modifying the

48 landscape and not intervening in time. However, if appropriate monitoring systems are implemented,

49 landslides can be properly controlled and, in some cases, predicted.

50   Human works may cause serious issues to potential unstable slopes, significantly changing its con-

51 figuration during the construction, (i.e. stability of the natural slope, man-made slopes, debris accumu-

52 lation during excavations, structures for slope reinforcements, etc.) affecting the overall stability of the

53 slope and the hosted structures and thus requiring adequate monitoring systems. However, the installa-

54 tion of permanent monitoring systems with sensors (e.g. inclinometers, strain gauges, crack meters,

55 Global Position Systems) or benchmarks (e.g. prisms for total stations) could not be sufficient since their

56 operation on a large part of the slope would be hindered by construction works.

57   In such scenario, remote sensing techniques represent an effective and low-cost monitoring system

58 in aid of civil protection authorities for rescue and recovery operations within landsliding areas (Giordan

59 et al.; 2013; Plank et al.; 2016; Frodella et al.; 2018) and an important tool for the reduction of risks

60 connected to the construction and activity of infrastructures at the same time (Bozzano et al., 2010;

61 Strozzi et al., 2011; Herrera et al., 2013; Ciampalini et al., 2014; Infante et al., 2017).

62 Differential Interferometric Synthetic Aperture Radar (DInSAR) analysis has shown to be a cost-effec-

63 tive and time-efficient alternative for mapping surface deformation over wide areas with millimetric

64 accuracies compared to conventional monitoring techniques (Tofani et al., 2014; Di Martire et al., 2016;

65 Bonì et al., 2017; Confuorto et al., 2017; Dong et al., 2018).

66 DInSAR allows measuring ground deformation by analyzing the phase difference between multiple SAR

67 images acquired over the same area at different times and from different orbital positions (hereafter

68 referred to as temporal and spatial baselines, respectively) (Rosen et al., 2000). However, they cannot

69 completely substitute conventional methodologies, due to the inapplicability of DInSAR in slopes i)

70 without stable reflectors, ii) unfavorable to satellite view, iii) with rapid events (e.g. rapid landslides or

71 sinkholes) (Wasowski and Bovenga, 2014). DInSAR is widely used for monitoring of natural phenom-

72 ena, while applications on consequences due to construction works can be found in Strozzi et al (2009),

73 whose work is based on the impact of the installation of mobile barriers for Venice coastland stability,

74 in Liu et al. (2014), which followed the deformation due to a tunneling process in Düsseldorf (Germany),

75 in Serrano-Juan et al., (2017), where DInSAR data were compared to leveling measurements for the

76 monitoring of urban underground construction in Barcelona, Spain or, more recently, in Milillo et al.

77 (2018), in which damage related to Crossrail tunneling in London was examined. Here, the results of

78 slope monitoring during and after the installation of remedial works within a landslide-affected area are

79 shown, in order to analyze their impact and their performance over the time.

80   Specifically, the Coherent Pixel Technique (CPT, Mora et al., 2003, Blanco et al., 2008, Iglesias et

81 al., 2015), has been exploited for studying the slope response to human interventions, installed in the

82 Quercianella hamlet, in the municipality of Livorno, with the aim of reducing landslide risk (Tuscany

83 Region, Italy), involved by the re-activation of a landslide in March 2011. The Livorno municipality has

84 been often harshly affected by natural hazards, and a last tragic episode occurred in September 2017,

85 where a water flood killed 8 people and destroyed several houses located close to a small stream, in the

86 aftermath of a severe storm.

87   Descending COSMO-SkyMed images were acquired (furnished by the local municipality of Livorno)

88 and used in the CPT processing, covering 6 years of monitoring (2011-2016). The CPT approach over-

89 comes the limitation of the Persistent Scatterers (PS) approaches, which demands a larger number of

90 SAR images to be reliable, typically more than 20, by exploiting the spectral properties of point-like

91 scatterers, referred to as Temporal Sublook Coherence (TSC) estimator (Iglesias et al., 2015). Hence,

92 spaceborne data have been compared with ground-truth information as to quantitatively evaluate Quer-

93 cianella slope stability and the impact of human interventions on it.

94   Because of the very complex pre- and post-intervention deformational scenario, difficult to outline

95 with punctual ground-truth data, an omni-comprehensive monitoring and modeling system was needed

96 to evaluate the stability conditions of the area involved by the remedial works.

97   Furthermore, the study also represented an inclusive source of information for the geotechnical ser-

98 vice company being in charge, to address and manage the phases subsequent the construction and the

99 remedial works within the landslide-affected area.

100 ~~The work is outlined as follows: the geological and geomorphological settings along with geotech-~~
101 ~~nical issues occurring at Quercianella, are presented in section 2. Section 3 describes the data used for~~
102 ~~the landslide investigation. Thus, the work is divided in 3 parts: Section 4.1 provides the results related~~
103 ~~to the pre-remedial work phase; Section 4.2 describes the technical configuration and the impact of the~~
104 ~~remedial work, Section 4.3 is referred to the post-remedial work monitoring and slope behavior, while~~
105 ~~the last section provides a general description about the latest trend in the implementation of integrated~~
106 ~~monitoring systems for landslides movements. Finally, discussions and conclusions of the paper are~~
107 ~~given.~~

2. Geological and geomorphological setting

109   The Quercianella hamlet is located about 5 km south of Livorno city, on the Tuscany coast, exposed

110   along the Tyrrhenian Sea at average elevation of 22 m above sea level. Livorno is located exactly south

111   of the Arno river mouth. The Arno path crosses a basin subsided by tectonic ridges, in NW-SE Apen-

112   nines direction. The municipal area of Livorno extends in a geologically complex territory, due to dif-

113   ferent units, according to the lithology and the tectonic arrangement. Three different complexes crop out

114   in Livorno, from the bottom to the top: i) arenaceous rocks of the Tuscany Series, with clayey-marly

115   formations and calcareous and siliceous strata and ophiolitic complexes, belonging to the Ligurian Suc-

116   cession; ii) Neogenic complex, represented by lacustrine and marine sediments of Upper Miocene; iii) a

117   Quaternary complex, made of marine sediments of the coastal strip. The structure of the Livorno Moun-

118   tain is made by allochthonous complexes of the Ligurian Domain, from Jurassic to Paleocene in age,

119   namely rocks belonging to tectonic units dislocated during the Apennines formation during the Miocene.

120   The lithologies outcropping in the Botro Trench are related to different weathered grade of the same

121   unit: the Palombini Shale Formation, belonging to the Ligurian Succession (PSF; Lower Cretaceous)

122   (De Capoa et al., 2015) (Figure 1). The PSF is constituted by blue-green, frequently sicilified marls and

123   marly limestone with limestone levels becoming more prominent toward the bottom and represents a

124   part of the sedimentary cover of the Ligurian Accretionary Complex (Plesi et al., 2002). The depositional

125   environment is that of a deep ocean, however, frequent terrigenous contributions from turbid currents

126   are evident according to more accurate sedimentological analyses (De Capoa et al., 2015). The old in-

127   habited area of Quercianella is on a flat coastal plain shaped by the marine activity, while the urban

128   growth of the last decades focused on the surrounding hilly areas. The sector affected by the landslide

129   movement is part of a hilly area, with a N-facing slope, at an altitude between 25 and 85 m a.s.l. The

130   landslide under investigation affects five buildings along Via Falcucci, in the eastern portion of the set-

131   tlement of Quercianella, where a dozen people live permanently. The displacement concerns the left

132   bank of an ENE-WSW oriented Quaternary valley, the Botro Trench, which has been V-shaped by the

133   Botro river. It can be considered as a reactivation of an old movement reported in the Hydro-Geomor-

134   phological Setting Plan (HSP, 2012), previously dormant, located between the ridge and the Botro

135   Trench, which starts as rotational slide and evolves in a translational slide in the foot area, (Cruden and

136   Varnes, 1996). The active landslide is 180 m long and has a width of about 100 m. Several traces of the

137   re-activation have been found, such as tension cracks and little scarps within the landslide body. From a

138   climatic point of view, Livorno area is in a warm and temperate climatic setting, with dry summer and

139   humid winter periods, and with an average annual rainfall of 800 mm ca. (Hydrological Tuscany Service

140   - http://www.sir.toscana.it/pluviometria-pub).
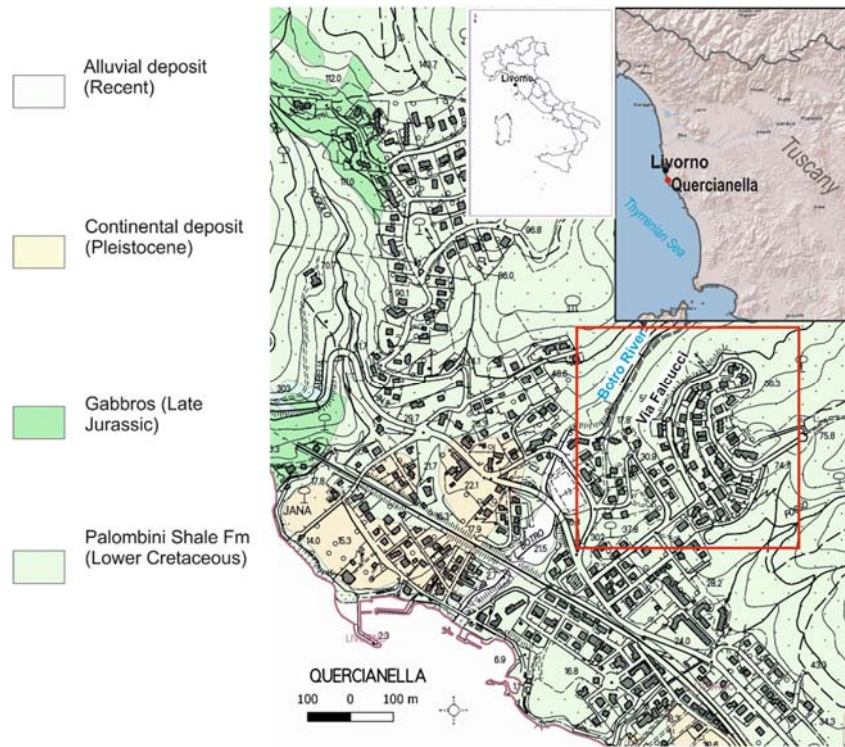
Figure 1. Geological setting of Quercianella hamlet. In the red square, the exact location of the
landslide-affected sector.

3. Materials and Methods

The geological and geomorphological setting of Quercianella slope described in Section 2 has led to
design specific geotechnical site investigations and a site-specific monitoring system to assess the sta-
bility conditions of the slope of interest made of 9 boreholes installed in 2011 and equipped with both
inclinometers and piezometers, which assisted the design and location of the drainage well placed in the
inhabited area with the aim of reducing pore pressure. Figure 2 summarizes the progression of the oper-
ational phase and the related monitoring system in Quercianella. These investigations, following the
landslide reactivations in 2011, are part of the slope characterization and mitigation interventions ap-
proved and financed by the Livorno municipality. Two monitoring campaigns have been completed in
the Quercianella area: the first measurements campaign was carried out in 2011, allowing the design of
the mitigation works, however related data have been partially made available by the company in charge.
The second one, started in 2013 was useful to monitor the effect of remedial interventions as to improve

7

156   slope stability; the surface movements were measured by CPT-TSC technique, starting from 2011. The

157   sparse vegetation cover, along with the consistent number of buildings and infrastructures, especially in

158   the crown area, and the rate of the slope movements greatly affected the distribution of ground investi-

159   gations and the selection of the CPT-TSC method, particularly suited for urban scenarios (Iglesias et al.,

160   2015). Indeed, the CPT-TSC performs an appropriate selection of pixels showing a correlated spectrum

161   in the temporal domain, without any compromise between quality of the estimation and spatial resolution

162   of standard DInSAR techniques (Ferretti et al., 2001; Berardino et al., 2002, Lanari et al., 2004).

163
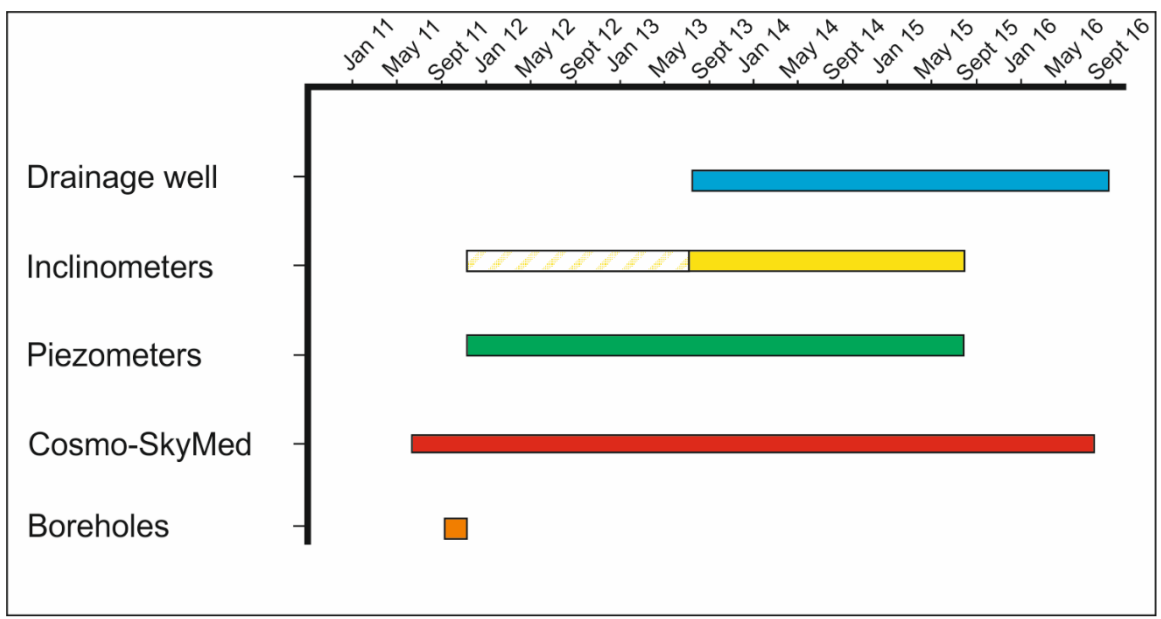
Figure 2. Timesheet of the operating drainage well and of the monitoring system in Quercianella area. Inclinometers readings before September 2013 are not available.

166   *3.1 Conventional Geotechnical monitoring*

167   The geotechnical monitoring was necessary to analyze the landslide movement and to follow the

168   remedial work performances, before, during and after its implementation. The monitoring program had

169   as main objective the examination of the efficacy of the intervention through the analysis of pore pressure

170   and deep displacements. Geotechnical monitoring has benefitted of nine boreholes completed in 2011,

171   as to define the geological model of the area. The boreholes have been carried out through either contin-

172   uous coring for undisturbed soil sampling or core-destruction drilling techniques to be successively

173   equipped with piezometers and inclinometers, at depths variable from 6 to 35 m.

174   For the monitoring of the subsurface horizontal movements, three inclinometers have been installed

175   (I1, I2, I3), respectively close to the drainage well and along Via Falcucci, I2 in the northern part and I3

176   in the SE sector (Figure 3). For the characterization of the hydrogeological setting of the study area, 6

177   piezometers have been installed in 2011 and were used also in the 2013 monitoring campaign: all of

178   them are Casagrande piezometers and are spread along Via Falcucci area, from S to N. ~~The monitoring~~

179   ~~of the hydrogeological of the study area allowed obtaining more complete information about groundwa-~~

180   ~~ter evolution, defining the most suitable intervention for water regulation and draining in landslide af-~~

181   ~~fected areas and finally monitoring slope conditions.~~

182
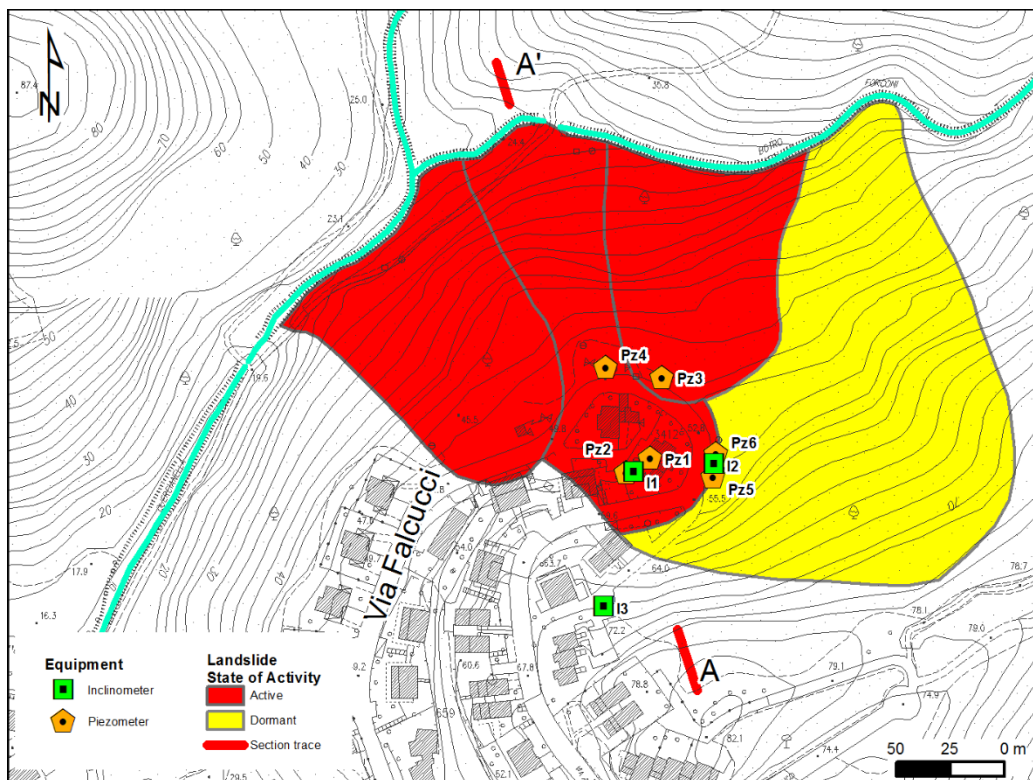
183   **Figure 3.** Location map of the instruments installed in the study area. Landslide reported are taken

184   from Hydro-geomorphological Setting Plan of Tuscany Region (2012).

Instrument	typology	Depth b.g.l., m	Casagrande cells depth, m b.g.l.
I1	*inclinometer*	*24*	*-*
I2	*inclinometer*	*15*	*-*
I3	*inclinometer*	*35*	*-*
Pz1	*piezometer, C*	*34*	*20*
Pz2	*piezometer, C*	*20*	*10*
Pz3	*piezometer, C*	*7*	*6*
Pz4	*piezometer, C*	*15*	*15*
Pz5	*piezometer, C*	*15*	*15*
Pz6	*piezometer, C*	*6*	*6*

185

186   **Table 1.** Instruments installed in Quercianella area. C stands for Casagrande piezometer.

187

188   *3.2 SAR dataset and processing*

189   Thanks to an agreement between the Livorno Municipality and the Italian Space Agency (ASI), 59

190   very high-resolution descending Stripmap images, acquired by COSMO-SkyMed (CSK) constellation,

191   have been made available, spanning between May 2011 and August 2016. They were acquired by the

192   X-band (i.e. 9.6 GHz center frequency with a maximum radar bandwidth of 400 MHz and 3.1 cm wave-

193   length) CSK-1 and CSK-2 sensor onboard at altitudes of ∼800 km above the Earth's surface, along sun-

194   synchronous polar orbits. The image stack covers an area of 40 km by 40 km, and the slant range and

195   azimuth pixel spacing of the scenes are 3×3 m. The Line of Sight (LOS) characterizing the stack has an

196   incident angle of 29º (with respect to vertical) referred to the centre of the scene, and the satellite ground

197   track is tilted approximately 8.5° with respect to the N-S direction at the latitudes of northern Italy. The

198   nominal repeat cycles of each CSK sensor are 16 days, meaning that archive for the Quercianella area is

199   quite dense for the 6 years under investigation. A subset of the full image frame was selected to cover

200   the area of interest, by clipping the coregistered scenes to 1,000 pixels in range and 1,900 in azimuth,

201   which corresponds to ~17 km^2. The resulting average coherence of the processed subset was generally

202   quite high (0.6, which corresponds to a phase standard deviation of 20°) for most of the scene and only

203   forest areas, along the NE sector of the clips, show low coherence (i.e. between 0 and 0.4). The images

204   have been processed through CPT technique by exploiting the Temporal Sublook Coherence (TSC)

205   method for the pixel final selection, developed by researchers at the Universitat Politecnica de Catalunya

206   in Barcelona (Iglesias et al., 2015). ~~The latter allows selecting point-like scatterers analyzing the spectral~~

207   ~~properties of the scattered signal. Hence, in this case, the pixel selection is carried out exploiting the~~

208   ~~spectral properties of point-like scatterers.~~

209   Since the data multilooking is not required in this case, the resolution of the original image is preserved

210   during the detection of PS. For this reason, this method is typically addressed as full-resolution PS but,

211   contrary to the PS technique, is able to work even with a limited number of images. Further description

212   of the CTP-TSC technique can be found in Iglesias et al. (2015).

213   From the availability of the abovementioned stack of images, 205 interferograms have been generated,

214   for the processing, characterized by maximum spatial baseline of 350 m and a maximum temporal base-

215   line of 300 days.

216   The distribution of PSs has been gathered, where positive velocities indicate surface deformation

217   towards the sensor while negative deformation rates reflect movements away from the sensor.

218   LOS deformation rates between ±3 mm/yr (close to the sensitivity of DInSAR techniques) correspond

219   to motionless areas (Colesanti and Wasowski, 2006).

220   In order to match both inclinometer and DInSAR data, inclinometer displacements have been re-

221   projected along the LOS (see Section 5). Such projection has been achieved through the following equa-

222   tion (Di Martire et al., 2015):

$$D_{LOS} = -Dsin\theta \cos(\alpha - \varphi)$$

(1)

Where D_{LOS} is the inclinometer displacement along the LOS and D is the inclinometer displacement, θ is the incident angle of the CSK data, φ the heading angle (azimuth of the LOS – 8.5°) and α the azimuth of the inclinometer.

4. Results

4.1 Pre-Remedial work phase

~~In March 2011, an instability event occurred on the north dipping slope of the Fosso Botro reactivated at a height between 22 m and 55 m above sea level (a.s.l.), which involved buildings and other man-made artefacts located in Via Falcucci. Geomorphological surveys and stereoscopic aerial photo interpretation of the 1975 and 1994 pairs (acquired from the Italian Military Geographic Institute) estimated that the movement affected a portion of a former dormant landslide.~~

~~The slope angle of the area, derived from a DEM (Digital Elevation Model) with a spatial resolution of 10 m (TINITALY project, Tarquini et al., 2007, 2012), ranges from 5° to 25°, with an average value of 10° and maximum values reached in the upper portion of the landslide, where the main scarp is located.~~

~~Such investigations have established that the phenomena consist in a re-activated landslide (HSP, 2012) starting as rotational slides and evolving in translational slides in the foot areas, according to Cruden and Varnes classification (1996), placed 180 m away from the crown areas. The total width ranges from 80 m of the main scarp to 250 m of the toe.~~

4.1.1 Definition of the geological model

In March 2011, an instability event occurred on the north dipping slope of the Fosso Botro reactivated at a height between 22 m and 55 m above sea level (a.s.l.), which involved buildings and other man-made artefacts located in Via Falcucci. Geomorphological surveys and stereoscopic aerial photo

247 interpretation of the 1975 and 1994 pairs (acquired from the Italian Military Geographic Institute) es-

248 timated that the movement affected a portion of a former dormant landslide.

249 The slope angle of the area, derived from a DEM (Digital Elevation Model) with a spatial resolution of

250 10 m (TINITALY project, Tarquini et al., 2007, 2012), ranges from 5° to 25°, with an average value of

251 10° and maximum values reached in the upper portion of the landslide, where the main scarp is located.

252 A geotechnical monitoring was necessary to design the remedial work ~~performance~~. The monitoring

253 program had as main objective the investigation of ground water table and deep displacements ~~the effi-~~

254 ~~cacy of the intervention through the analysis of pore pressure and superficial and deep displacements.~~

255 Geotechnical monitoring has benefitted of nine boreholes installed in 2011, as to define the geological

256 model of the area and therefore to better design the drainage well, completed in August 2014. Piezome-

257 ters in the pre-design phase identified a single water table level, with direction parallel to the slope (see

258 Section 4.3.1 and Figure therein).

259 The lithological analysis of the boreholes executed in the geotechnical campaign shows ~~that~~ the fol-

260 lowing stratigraphic setting (Figure 4):

261 1. Active landslide deposits made of beige sandy silts and heterometric lithic fragments. This

262   layer has a maximum thickness of 10 m, according to the boreholes Pz4 and I1.

263 2. Ancient landslide deposits characterized by a succession of limestone and marly limestone

264   deposits within a grey marly and clayey matrix. This layer has a thickness ranging up to 6 m,

265   along the borehole I1.

266 3. Weathered portion of the PSF, represented by thinly foliated marls and limestone boulders

267   into clayey sediments. This layer has a thickness ranging up to 20 m, referred to the location

268   of the borehole I3.

269 4. PSF bedrock, consisting of blue and dark green marls in a clayey succession from a depth of

270   25/30 m from the ground level, interbedded with crystalline, marly or siliceous limestones at

271 deeper levels. As a consequence of intensive tectonic activity associated with the Alpine oro-

272 genesis, this formation is characterized by a high degree of structural complexity represented

273 by disarranged bedding and scaly structure of shales (Elter et al., 2003; Principi et al., 2004).
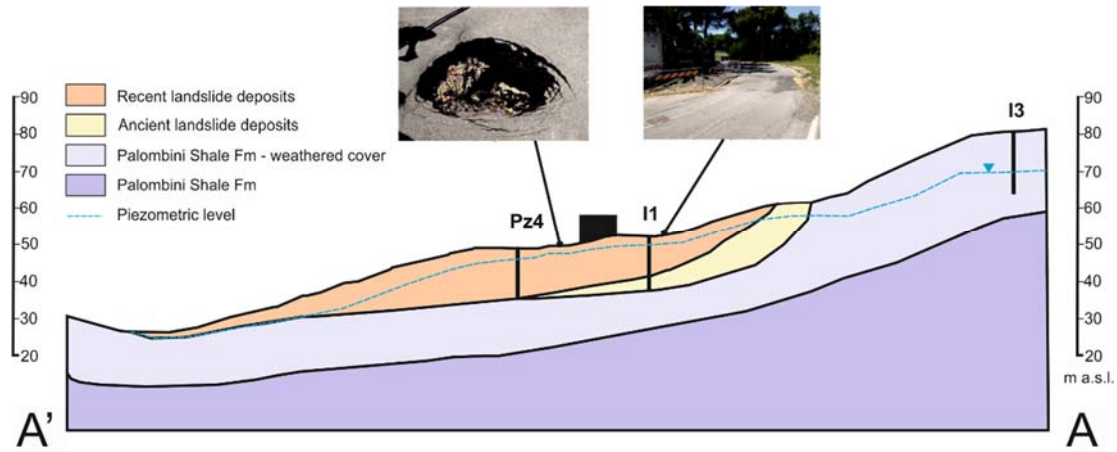
Figure 4. NNW-SSE geological cross section of Quercianella slope. The A-A' section trace is in Figure 3. Photos show damage reported along the slope.

277 The data collected suggest that the current movement corresponds to the reactivation of the upper

278 landslide deposits, as part of an older and wider phenomenon previously mobilized.

279 A high geomorphological risk is associated to this area, according to the Hydro-geomorphological

280 Setting Plan (HSP) of the Tuscany Coast Authority (2012).

281 Moreover, representative samples were collected from the various boreholes, and laboratory testing

282 were performed (triaxial test, shear stress test, etc.) integrating these results with field testing, such as

283 SPT (Standard Penetrometric Test) test. On the base of the results of such tests, a geotechnical model

284 has been defined, summarized in table 2, where the main parameters are reported, such as γ (volume

285 weight), Φ' (peak friction angle), c' and c_u (drained and undrained cohesion, respectively). In the specific

286 case of c', it is assumed constantly as 0, simulating the possible scenario where the re-activation of the

287 landslide is caused by a rise of the piezometric level.

288 Thus, a back-analysis slope stability test was performed to assess the safety condition of the slope

289 considering the original pre-event slope geometry obtained from the DEM of the area and a slip surface

290 located at about 10 m b.g.l. (at the boundary between recent and ancient landslide deposits), performed
291 using the Morgenstern and Price method (Morgernstern and Price, 1965), referred to limit equilibrium
292 condition, implemented in the SLOPE software (Geostru®). The residual friction angle which led to limit
293 equilibrium (FS=1), along a strip containing the slip surface identified is 16°. Once validated the ge-
294 otechnical model in failure condition, considering the interaction between ground and structure and the
295 piezometry of the area, a Finite Element Model (FEM) analysis has been implemented, aiming at the
296 more detailed definition of the condition which potentially could have led to failure, through the software
297 PLAXIS-2D AE (Plaxis®). This code is implemented with the possibility of simulating the behaviour of
298 the terrain by using different constitutive models of the slope. For all the different geological units of
299 the area, an elasto-plastic behaviour has been assumed, and the Mohr-Coulomb constitutive model has
300 been adopted, where the material has a linear isotropic elastic style for the tension states within the
301 strength envelope of Mohr-Coulomb, as well as it has a plastic style for tension states along the envelope.
302 The same parameters and slope configuration of the Morgernstern and Price analysis have been here
303 considered, and the model has been discretized using triangular elements (Figure 5).

Geolithological Unit	Thickness (m)	γ (kN/m^3)	φ' (°)	c' (kPa)	c$_u$ (kPa)
Recent and ancient landslide deposits	12	19	20	0	20
Slip surface strip	2	19	16	0	20
Weathered Palombini Shale Fm	13	20	24	0	50
Palombini Shale Fm	>25	22	24	125	100

304

305 **Table 2.** Physical-mechanical properties of the geolithological units obtained through the different
306 tests.

307 The analysis of the slope condition before intervention is structured as follows:

1. Assessment of the initial tension state, where the initial tensions are generated using the generation procedure of the initial tension by increase of the gravity.

2. Assessment of the global safety factor of the slope without considering the piezometric level. In this case, the strength values of tan φ and c of the terrain are reduced until failure of the slope. The global Safety Factor ΣMsf is used to define the values of terrain strength in a certain stage of the analysis:

$$\sum Msf = \frac{tan\Phi_{input}}{tan\Phi_{reduced}} = \frac{c_{input}}{c_{reduced}}$$

Where the input parameters are related to the properties of the materials and the reduced ones to those used for the analysis. At a first stage, ΣMsf is equal to 1, as to set all the strength parameters to their original values. The final step of the analysis is when the failure of the slope is simulated. In this case the Safety Factor is

$$SF = \frac{available\ strength}{failure\ strength} = \sum Msf\ during\ failure$$

The reduction approach leads to a definition of the slope SF similar to that calculated with the limit equilibrium method. In the case of Quercianella slope, the SF= 1.42, therefore, the slope is stable when water is absent.

3. Assessment of the Safety Factor considering the piezometric level. In a first phase, the piezometric level is reconstructed according to previous data, collected before the beginning of the remedial works. Thus, the analysis has been made through filtration motion, where a constant hydraulic load is defined, specifying a constant distribution and without varying the hydraulic load with time. The plastic point distribution shows a mass movement affecting the superficial part of the slope and a SF, obtained reducing Φ and c as in the previous case, of 0.98, thus

332   demonstrating the instability of the slope with the piezometric level indicated previously.

333
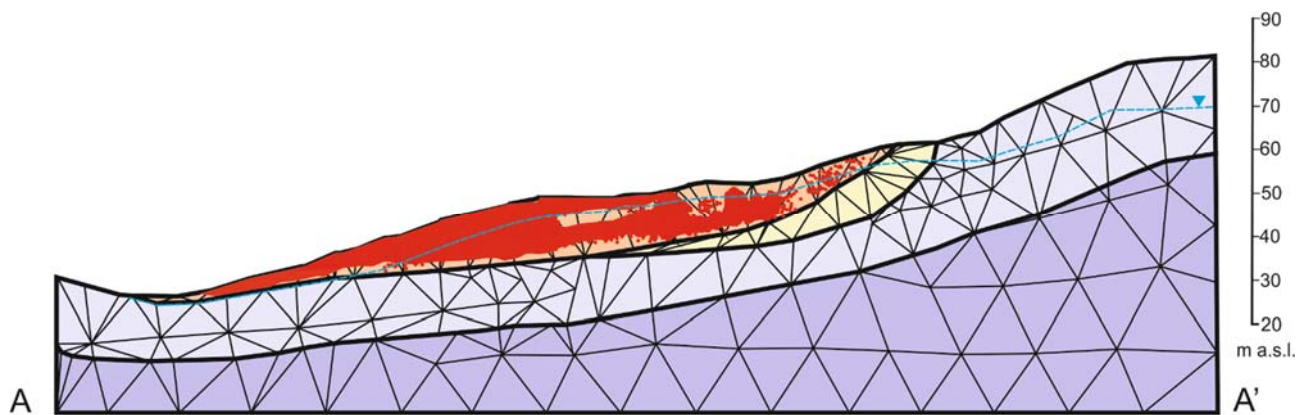
334   **Figure 5.** NNW-SSE geological cross section of Quercianella slope with the distribution of

335   triangular elements and plastic points according to the FEM analysis. Blue-dashed line in-

336   dicates the ground water level.

337 *4.1.2 CPT-TSC monitoring*

338   To observe and analyse the movement related to the activation of the Quercianella landslide, CPT

339 algorithm was selected and applied on images spanning between May 2011 and July 2013.

340 Thus, the elaboration of the descending data (Figure 6) shows a displacement pattern characterized by

341 maximum value of velocity of -11.7 mm/yr, which has been registered nearby the detachment area, as

342 well as other PSs with considerable velocities (-10 mm/yr in average) are located along the main scarp

343 of the landslide and over the northernmost building, one of the most damaged by the phenomena. Other

344 PSs showing displacement are within the active landslide boundaries, while stable PSs are in the southern

345 area of Quercianella, in an area without significant movements. Such analysis confirms the active state

346 of the landslides detected in the field and through aerial photo-interpretation, providing a first state-of-

347 the-art of the area.

348
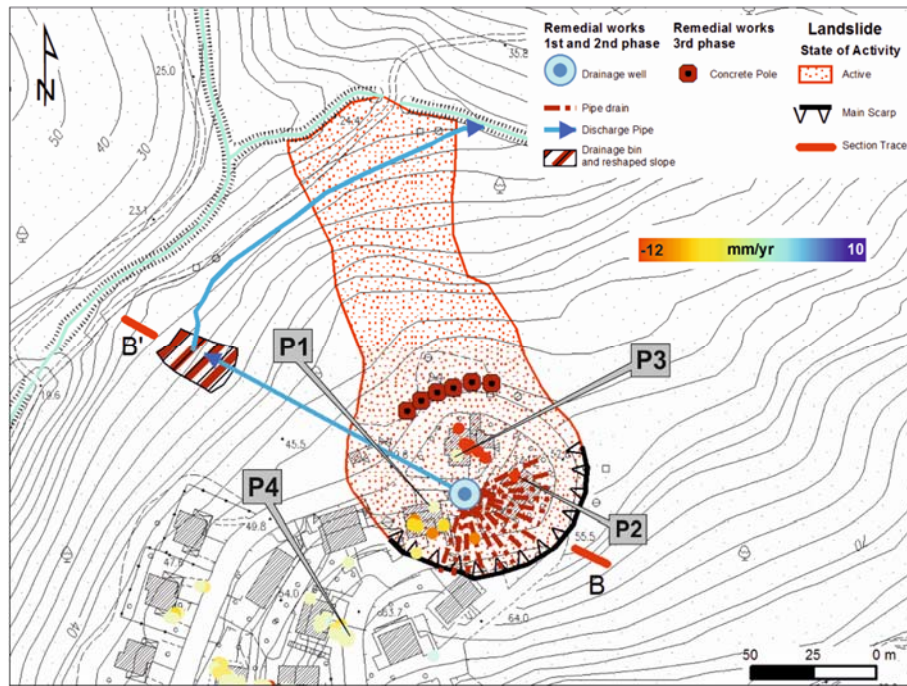
Figure 6. Displacement rate map related to the time span May 2011 – July 2013 along with the design of the remedial works.

4.2 Remedial works

The lack of water surface regulation in Quercianella, due either to the scarce maintenance of existing collection systems, but mostly to the intense urbanization, is strongly responsible for the reactivation of the Via Falcucci landslide. To reduce the pore pressure acting on the sliding surface, a deep drainage well intervention was chosen, thus increasing shear strength of the soil: the modification of the piezo-metric regime in the landslide area allows to increase the safety of a sector of the slope affected by the landslide movement. The design phase consisted in a new slope stability analysis, where the drainage well has been placed in the landslide affected-area. According to the simulation, the stabilization of the area has been obtained lowering the ground water table to about 10 m b.g.l., reaching a SF equal to 1.26 in the upper part of the slope, while in the lower part a further intervention has been designed, being still unstable.

The overall framework of the interventions, considering the setting of the area, has been divided into two consecutive phases:

364   1) installation of hydraulic surface regulation works and of a drainage well and execution of parallel

365   tubular discharge system in the lower part of the slope, to pump the water out of the landslide area;

366   2) execution of further structural works according to the effects following the interventions of the

367   phases 1 ~~and 2~~, necessary to further increase the safety factor for the slope stability.

368   ~~To reduce the pore pressure acting on the sliding surface, a deep drainage well intervention was chosen,~~

369   ~~thus increasing shear strength of the soil: the modification of the piezometric regime in the landslide~~

370   ~~area allows to increase the safety of a sector of the slope affected by the landslide movement. To this~~

371   ~~aim, a deep drainage system has been proposed during the design phase in the area above Via Falcucci~~

372   ~~(where most of the damaged infrastructures are located).~~

373   In detail, the drainage system consists of a well and draining tubes arranged in a radial pattern. The

374   well has been placed in a barycentric position with respect to the Via Falcucci area, thus being in the

375   perfect center and in the deepest portion of the landslide, and easy to access as well. The geometry of

376   the well, having a diameter equal to 5 m and height equal to 13 m, has been made according to several

377   factors, such as: compatibility with the site, necessity to contain a drill to install micro-drains, require-

378   ment of keeping the micro-drains out of the bedrock and avoid the damaging of the well and the drains

379   due to the movements of the most superficial layers; the need of placing the drains to a depth sufficient

380   to reduce the pore pressure and improve the slope safety conditions.

381   Two levels of drains have been implemented to obtain such goal: the first one at 10.5 m b.g.l. and the

382   latter one at 12.5 m from the ground, having a length of 30 or 40 m, diameter equal to 90 mm and

383   inclination of 5% or 10%. As to maximize the drainage efficiency, tubes have been placed in the first

384   meters of the weathered bedrock, avoiding the penetration into the bedrock.

385   The disposal of the water collected inside the well has been achieved by gravity through a HDPE

386   (High-Density Polyethylene) discharge pipe with a nominal diameter of 110 mm and a length of approx-

387   imately 105 m, placed at a depth of about 13 m from the ground level, with a slope towards the valley

388   equal to 0.5%, implemented through the Directional Horizontal Drilling technique. After the installation

389   of the pipeline, a slope sector outside the landslide area has been reshaped, where a water collection

390 manhole was placed, used to deliver water to the Forconi Botro, through a channel characterized by a

391 trapezoidal section with base wider than 1.5 m and depth of 1 m, coated with geocomposite to limit

392 erosional processes, length of the order of 160 m and maximum slope of 3%. In Figure 6 the areal con-

393 figuration of the system is showed, cross-section of Figure 7 summarizes the scheme of the works, while

394 Figure 8 displays the main features of the drainage well.

395 As regards the interventions following phase 1, remedial works have been designed, including the con-

396 struction of columns of consolidated soil, with a diameter of 400 cm at a distance of 35 cm, through the

397 deep mixing technique, affecting the most weathered soil cover for a depth of the order of 12 m from

398 the g.l. The choice to operate this type of consolidation allows the terrain-cover interface to be water-

399 proofed and to increase the stiffness of the ground around the well, contributing to the stability of the

400 work and to a significant reduction of the pressures induced by landslide on the wall of the well. More-

401 over, a series of reinforced concrete bulkhead of poles has been designed in the northern sector of Via

402 Falcucci, as to stop the movement and save the man-made artefact and the road in that area.

403 Nowadays, the works related to the second phase have not started yet.

404
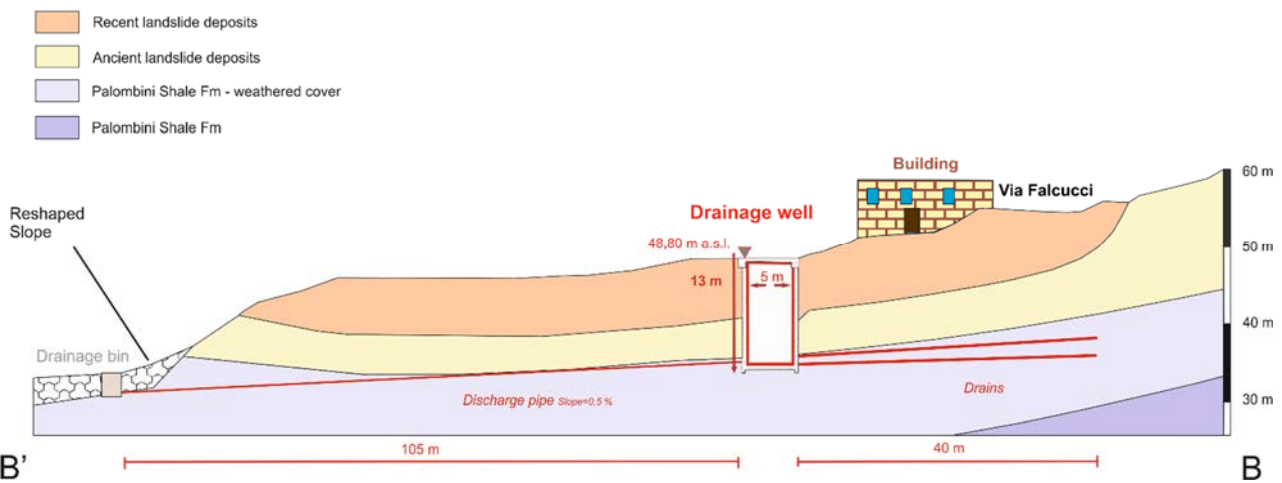
405 **Figure 7.** Cross-section of the landslide-affected slope sector showing the drainage well and the re-

406 lated features. Section trace location is in Figure 6.

407

408
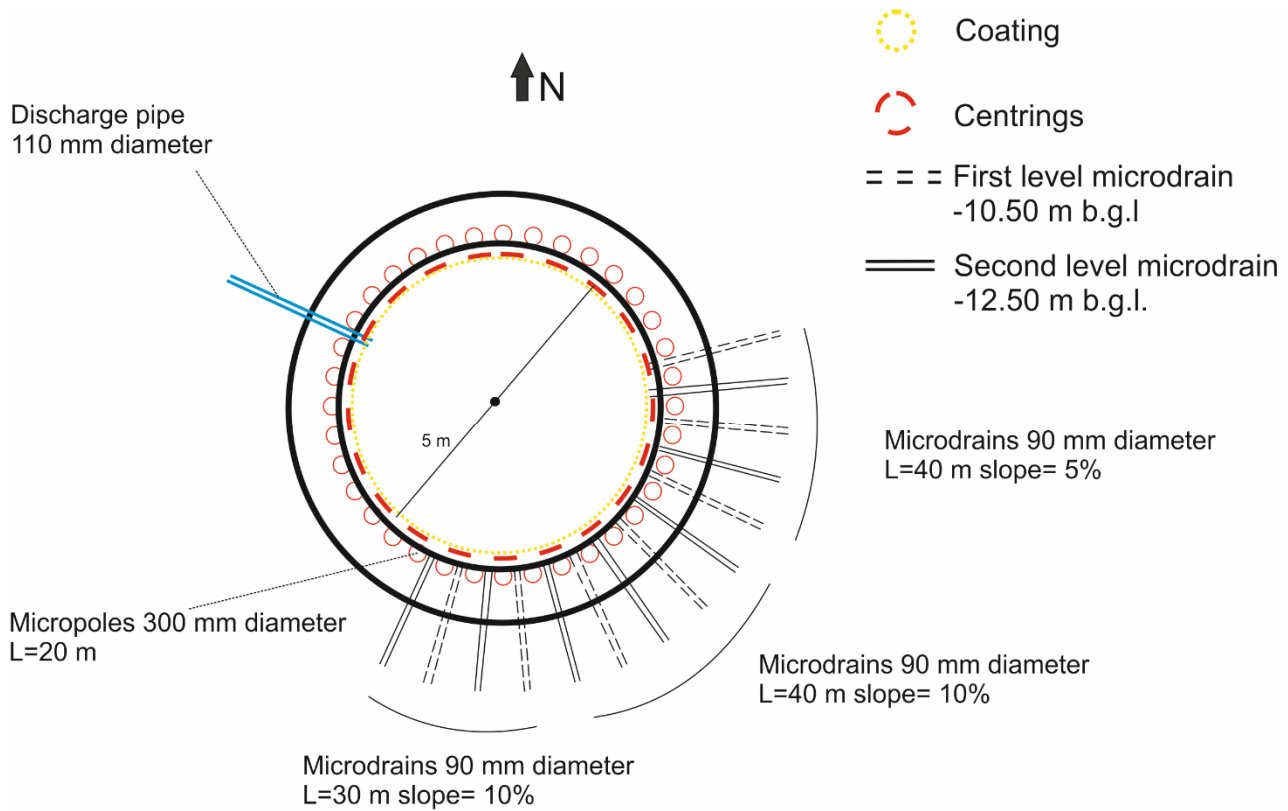
Figure 8. Scheme of the drainage well.

4.3 Post-Remedial work phase

4.3.1 Geotechnical Monitoring

Piezometric measurements show the presence of a water table surface with a direction parallel to the slope, at an average depth between 1 and 5 m from the ground level, at the beginning of the measurements from August 2013, when the second monitoring campaign has started. ~~The trend evidenced in Figure 9, shows the effects of the installation of the first PVC pipes in September 2013.~~ It is worth to mention that the installation of the drainage system lasted one year, from August 2013 to August 2014. During this year the ground water table fluctuations are caused by the excavation and the following setting up of the remedial works. Thus, the preliminary effects on the piezometry are visible in the time-span August-November 2014, where a decrease of ca. 2 m is reported in Pz1, the closer to the drainage well. This occurs most likely because the well has not gone to full capacity yet in November 2014. The

other piezometers registered a minor effect following the drainage of the area, due to the higher distance to the well, as shown by Pz3, Pz4, Pz5 and Pz6. Pz2 has provided only three measurements until its rupture. Furthermore, rainfalls occurring in the area during the remedial work construction period, seems to not to have a significant role in the ground water table level, except for work completion period (May-August 2014), where a slight decrease has been registered. ~~that, despite a limited effect on groundwater table soon after the installation of the first PVC pipes in September 2013, the pore-pressure has been reduced in the lower part of the landslide since October 2013. Hereafter, the piezometric level significantly decreased in piezometers Pz1, from -3.8 to more than -6.5 m b.g.l. in almost one year, starting from November 2013; in Pz3, from -5 m to -9 m b.g.l. in less than one year; piezometer Pz4 displays a sudden decrease from -2 m to -3.7 m in less than 3 months (August – October 2013); Pz5 and Pz6 show a very similar trend, being located in the same sector (E of the well), with a water table surface at -2 m b.g.l. in the months following the well implementation. Pz2 has not provided reliable results.~~
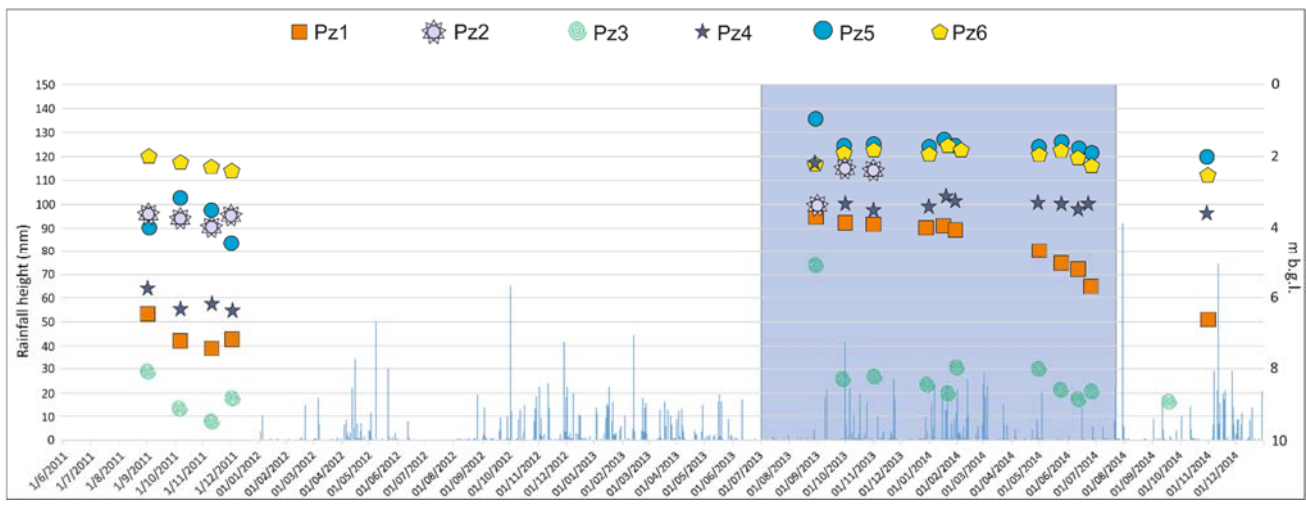
Figure 9. Piezometric measurements recorded in the whole time-interval of the monitoring. The blue-shaded area corresponds to the drainage system installation period. Daily rainfall data were acquired from Tuscany Region Hydrological sector web portal.

For the monitoring of the subsurface displacements, three inclinometers, located within the landsliding area, kept constantly providing measurements of the occurring displacements; for each of them, the corresponding depth of maximum displacement and the azimuth are shown in Figure 10. The following observations can be retrieved: for I1 and I2, a main slip surface is at about -10 m b.g.l. where maximum displacements of 18 mm and 70 mm were recorded over 2 years, respectively (Fig. 10a and 10b). I1 shows a first phase (between October 2013 and November 2013) with slight deformation (2 mm), followed by a sudden acceleration, until April 2014, reaching 12 mm of cumulative displacement; between April 2014 and September 2015 the displacement is of 7 mm. I2 shows a first phase with displacements of 28 mm, followed by a rapid acceleration between February and April 2014 (almost 20 mm) and thus a significative slowdown between April 2014 and September 2015 (about 12 mm). Moreover, both I1 and I2 showed a persistent displacement vector, NNW-oriented, with azimuth angle of 350 and 330°, respectively. I3 registered negligible movements in the time span September 2013 and December 2014, with cumulative displacement of 5 mm (Fig. 10c), being located outside of the active portion of the landslide. It is worth to point out that I1 and I2 registered ~~measures of deformation~~ displacements until September 2015, before their interruption. ~~because of higher and fast displacements which caused the rupture of the tubes.~~
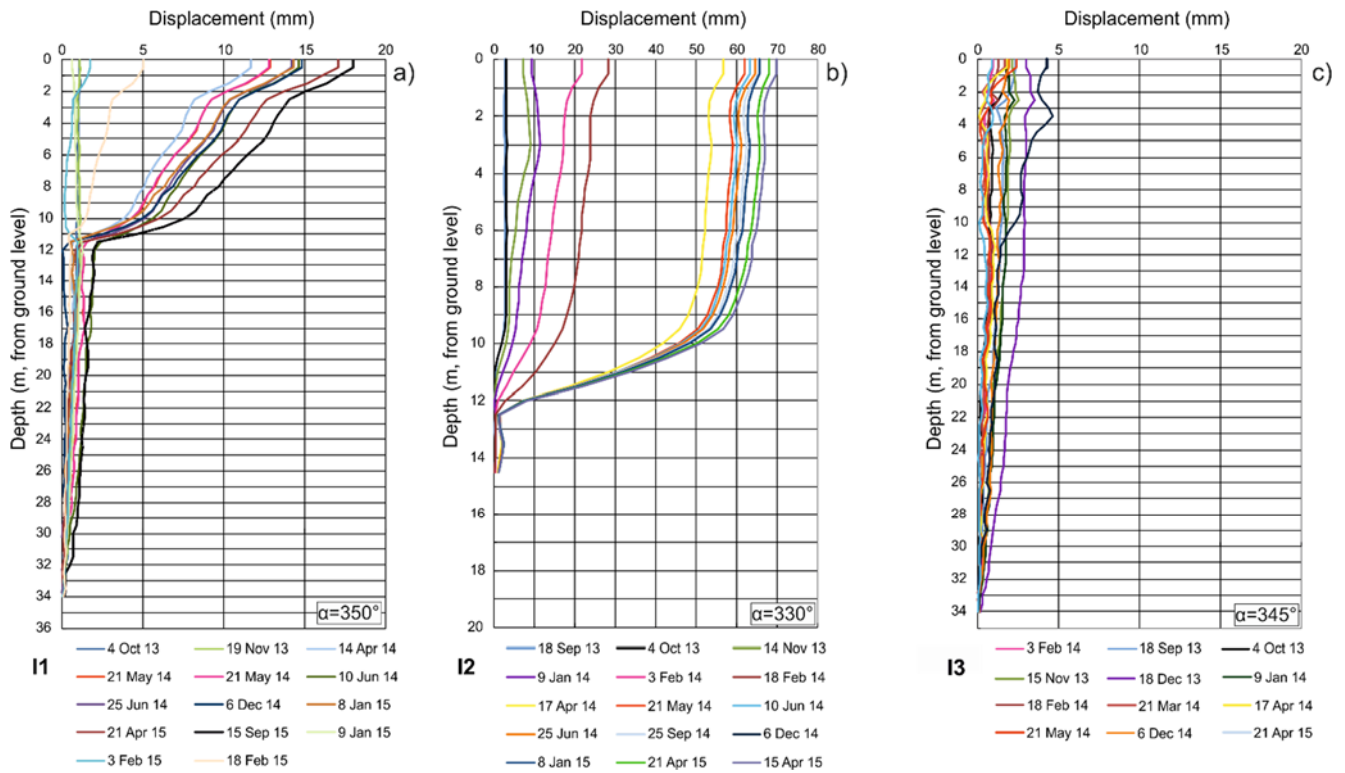
Figure 10. Inclinometric measurements recorded in the inclinometers installed: a) I1; b) I2; c) I3. In the box in bottom right, the azimuth angle of each inclinometer is reported.

4.2 CPT-TSC monitoring

The elaboration of the descending data, related to the post-remedial works phase, shows a displacement pattern characterized by an average velocity of |6.5| mm/yr among the 52 points within landsliding area. The maximum value, of -22 mm/yr, has been registered nearby the detachment area, as well as other PSs with considerable velocities (-18 mm/yr on average) are located along the main scarp of the landslide and over the northernmost building, one of the most damaged by the phenomena (Figure 11). As to analyze and to better interpret the landslide evolution, time series of displacement have been calculated and examined, considering the time span May 2011 - August 2016. To this aim, four points, located in different parts of the area of interest, have been considered: points P1, P2 and P3 are placed within the landslide boundaries, P4 is located southwards. The first three points show a homogeneous deformation pattern, where considerable final displacements are distributed for the time span October 2013 – August 2016, of 2.9 cm, 1.9 cm and 2.1 cm, in P1, P2 and P3, respectively (Figure 12). Further analyzing the

24

469   temporal evolution of the movement, a significant acceleration can be noticed at these 3 points, around

470   December 2013 and January 2014. Such events can be partially correlated to the still active landslide,

471   but mostly to the excavation and the installation of the drainage well during the remedial works, ended

472   across September 2014. After the intervention, a stabilization of the movements in the points P2 and P3

473   can be observed, showing a clear slowing trend from May 2014, as well as displacements of ca. 1.5 cm

474   are still registered in the point P1, thus showing still a deformation trend. As regards point P4, it shows

475   a linear stable trend in the whole time-span of the analysis, being located out of the moving area. For an

476   in-detail analysis of the time series of displacement, see Figure 12 and Section 5.
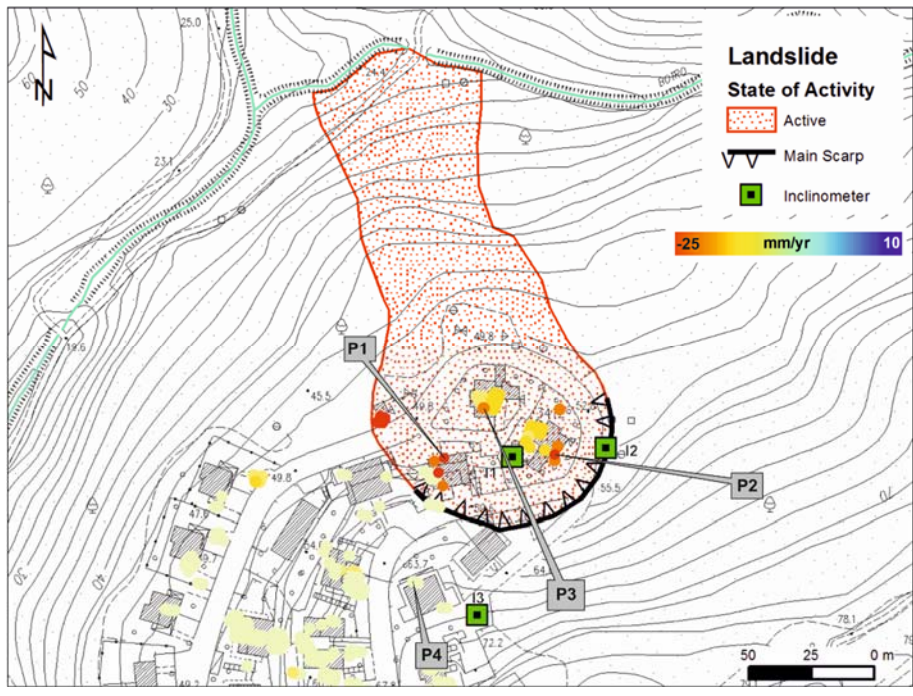
477

478   **Figure 11.** Displacement rate map related to the time span August 2013 – August 2016.
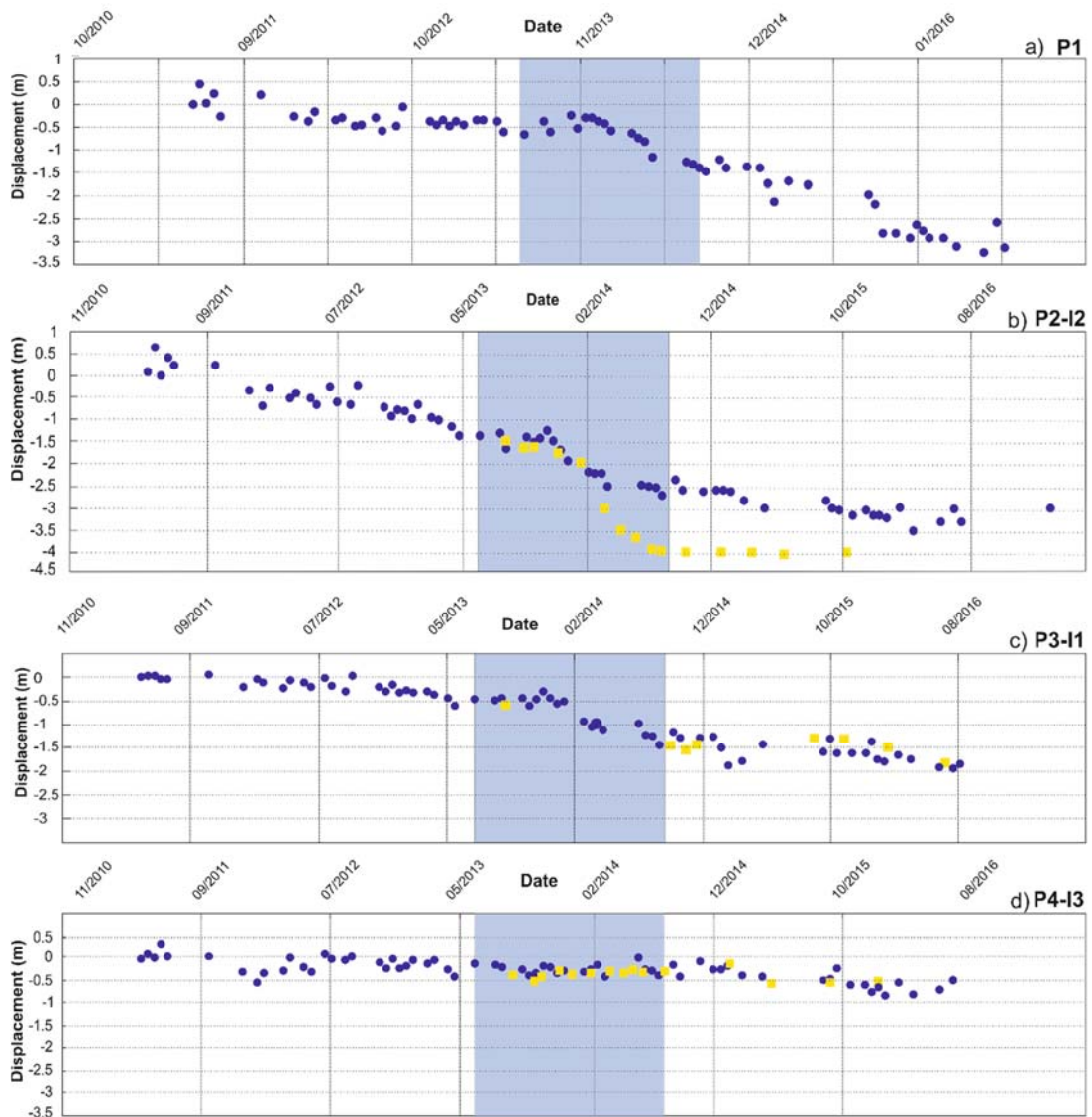
Figure 12. Time series of displacement by CPT processing (blue dots) and inclinometer data (yellow squares). The blue-shaded area corresponds to the installation period of the drainage well. Inclinometers were re-projected along the LOS (see section 3 for the description of the procedure adopted).

5. Discussion

The availability of a long-lasting dataset of SAR imagery permitted a complete monitoring and analysis of the landslide-affected area of Quercianella, a small hamlet of Livorno municipality, Italy. Different phases of the landslide characterization have been recorded: the first, during which landslides have been detected by DInSAR and it has been possible to define and update landslide boundaries, with the help of photo-interpretation and field activity, prior to the implementation of remedial works in the area;

26

the geological model was also defined, through the equipment of nine boreholes; a second one, referred

to the setting of remedial works, consisting in the installation of a drainage well and tubular drains, with

the aim of lowering the water table surface; the last one, where the performances of the drainage well

have been monitored, verifying the excavation first, and thus the stabilization of the slope. For the first

task, the following considerations have been done: Quercianella landslide was already known by munic-

ipal authorities, which started a monitoring campaign following the re-activation of March 2011, con-

sisting in both *in situ* and remote sensing measurements, to better design remedial work. Based upon the

evidence shown in this paper, boundaries and the state of activity of the Quercianella landslide, available

from the HSP of the Tuscany Coast River Basin Authority, have been updated, showing the clear dis-

placement pattern of the identified landslide in the Via Falcucci area. Moving downslope, the phenom-

enon evolves into a translational slide, as the landslide mass moves along a roughly planar surface with

little or no internal deformation, and the slide further transforms into an earth flow in the accumulation

area. Thus, the second and third part of the work highlights the different steps of engineering works,

consisting in the implementation of a drainage well, designed with the aim of decreasing the pore pres-

sure, and placed in a barycentric position with respect to the landslide, whose consequences have been

followed by the monitoring equipment of the area. DInSAR, piezometric and inclinometric data have

been integrated in this area to control the performances of the drainage system adopted to modify the

hydrogeological conditions, responsible for the landslide movement. According to the geological model

of the area, the chosen system consisted in a drainage well and draining sunburns-arranged tubes. Pie-

zometric measurements highlighted changes of the water table depth in the area close to the well, fol-

lowing the first phases of the excavation of the area, where several fluctuations are reported, hence fol-

lowing the activation of the drainage well (up to 2 m decrease in 5 months, during autumn), however

also confirming the necessity of further intervention, designed but still not realized, in the northern area,

down the valley, out of the well range, where no significant effect has been registered. Inclinometric

readings and PSs time series were in total agreement and both confirmed the displacement pattern of

Quercianella area.

As to confirm and compare the interferometric results so far commented, in fact, time series of displacement of PSs have been related to the displacement recorded by the closest inclinometers installed in the study area (I1, I2, I3).

Therefore, the two data show a nearly perfect agreement of points P3 and I1 (Figure 12c), highlighting the acceleration of the ground related to the beginning of the excavation (November 2013) and the following stabilization of the slope after the completion of the operation and the beginning of drainage operation (April 2014); points P4 and I3 also display a coherent trend between both data (Figure 12d), recognizing a nearly stable trend due to the higher distance from the active portion of the landslide depicted; finally, a certain difference is distinguishable in P2 and I2 (Figure 12b), whose dissimilarity can be connected to the extreme rapidity of the displacement in a reduced time span (3 cm in 2 months, among December 2013 and March 2014), recorded in the point P2, not allowing interferometric technique to correctly work, because of their inability to analyze rapid deformations in such a short amount of time, which induces a loss of coherence in the PS. This happen because the theoretical displacement detection threshold between two SAR images is $\lambda/4$ (where λ is the wavelength). Considering a λ of 3.1 cm for X-band and a time span of 16 days between two acquisition the maximum theoretical displacement rate would be about 2 cm in two months (Herrera et al., 2010).

Therefore, the installation of the drainage well and the consequent stabilization of the landslide-affected area have been constantly monitored by DInSAR, performing well not only in the monitoring of the displacement itself, as shown in section 4.1, but also controlling the installation (consisting in the excavation, the implementation and the coating) and the performance of the drainage well in the landslide-affected area (section 4.3). Moreover, the northernmost and downstream area of Quercianella, in Via Falcucci, resulted to be still affected by considerable displacement rates despite the installation of the drainage system, as observed in time series of point P1 (Figure 12a), in the timespan November 2014 – August 2016. This has confirmed the necessity of the implementation of the second phase.

This last aspect may open a new scenario for the already wide range of radar-based application. Most of the works regarding DInSAR methodologies, in fact, deal with the monitoring of natural hazards, such

as landslides (Di Martire et al., 2017; Bejar-Pizarro et al., 2017; Frodella et al., 2018); subsidence (Tessitore et al.; 2016, Bonì et al.; 2017), sinkholes (Fiaschi et al., 2017), or are related to monitoring of structures and infrastructures affected by one or more of the above-mentioned phenomena (Sousa et al., 2013; Arangio et al.; 2014, Di Martire et al., 2014; Infante et al., 2016; Tessitore et al., 2017); however, with this work the validity of such techniques also for the monitoring and the supervision of engineering works has been demonstrated, being able to suggest where and how intervene as to reduce the risk related to landslide phenomena, and thus revealing to be not only effective, but also time and money saving for stakeholders and customers. ~~Moreover, DInSAR has provided a full support for the whole time interval of the work, whereas inclinometric measurements were not available in the last phase, due to the rupture of the tubes.~~ Indeed, the costs of the two different monitoring system have been compared. The total cost associated to the analyses during the two stages (2011-2013 and 2013-2016) amount to 40.000 € for DInSAR, providing 59 displacement measurements (at least once a month) in the whole Quercianella area. It must be taken into account that CSK imagery acquisition for the Italian territory covered by Map Italy project is free of charge for public administrations (Sacco et al., 2015). The cost of conventional measurements is of more than 30.000 €, covering both the installation and the readings, which were about 20 in 5 year (2011-2015) of monitoring. Moreover, these have not provided complete information on the area, due to the restricted range of the punctual instruments on one hand, and due to the rupture of several instruments on the other.

DInSAR methods, therefore, can be considered a valid support also to the planning and the design of remedial works, suggesting where and how to do them, and controlling their performance over the whole necessary time.

6. Conclusions

The purpose of the presented application was to take a step beyond in the current state-of-the-art in the exploitation of SAR products as a support for a construction site where Differential Interferometry

SAR (DInSAR) results could eventually provide essential information for a correct planning of engineering interventions.

DInSAR data were used for the first time to analyze the effectiveness of engineering remedial works on a slope affected by a mass movement such as that of Quercianella (Livorno, Italy), before, during and after the interventions. The results can be considered relevant, taking into account the impact of the landslide on the inhabithed area and on the infrastructures and the necessity of ensuring appropriate safety conditions in favor of the dozens of family units threatened in the northern sector of the settlement.

The integrated monitoring system in this case has led the company, suggesting where to intervene as to mitigate landslide risk, showing also its interchangeability, where both inclinometer (due to ruptures) and satellite (due to unfavorable geometry of the slope) measurements have failed. In fact, as the excavations started for the installation of a drainage well, designed to reduce pore water pressure in the area, an acceleration of the slope movements and slight damage to buildings in the neighboring inhabited areas were observed, as well as SAR monitoring was able to follow slope response to beginning of the works, in September 2013. During this time-span, indeed, hydraulic regulation was achieved through the above-mentioned drainage well with a sunburns-arranged tubes; ~~followed by the execution of a tub-ular parallel drains in the lower part of the slope, and finally by the design of further remedial works to increase slope stability, whose original configuration and physic-mechanical conditions have changed due to the works;~~ moreover, a slope sector has needed the design of additional remedial works, consisting in bulkhead of poles, with the aim of stopping the deformation affecting the road. DInSAR results have represented a reference datum for the design of mitigation works and an important tool to guarantee safety during several phases of the construction activities as well.

In fact, displacement rates derived from the integrated measurements of DInSAR and inclinometers have been considered for the second stage of works when bulkheads had to be placed at the toe of Quercianella slope.

The availability of COSMO-SkyMed (CSK) short revisit time data has played a key role in our conclusions, while the reduced revisit capacity of orbiting satellites before the CSK mission was the most

591 serious gap for the extensive use of DInSAR information as an operational monitoring tool. In fact, a

592 critical issue for the application of remotely-sensed data in risk management applications has been gen-

593 erally represented by the limited capability of previous C-Band satellite radar sensors (e.g., ERS,

594 ENVISAT, ALOS PALSAR) to offer an efficient response to user's specific needs, in terms of image

595 resolution and accuracy, reaction time, latency of data and delivery time.

596 The enhanced temporal repetitiveness of the new constellations (i.e. TerraSAR-X, COSMO-SkyMed

597 and Sentinel-1), the unprecedented timeliness in terms of response time (quasi-real-time delivery of data

598 within a few hours of acquisition) and the flexibility of mission configuration (in terms of products

599 resolution and incident angle), now offer a time- and cost-effective opportunity to support two main

600 stages of the disaster risk management: the quantitative and qualitative assessment of the hazards and

601 the monitoring of remedial work performances. However, common limitations of DInSAR must be taken

602 into account, mostly related to the lack of reflectors, unfavorable geometry of the slopes or to the high

603 velocity of rapid landslides. Therefore, the integration of remote sensing techniques and site instruments

604 represents the best practice when planning remedial works, providing precise and rapid information

605 when dealing with risk-reduction and safety increase in landslide-affected areas.

References

Arangio, S., Calo, F., Di Mauro, M., Bonano, M., Marsella, M., Manunta, M., 2014. An application of the SBAS-DInSAR technique for the assessment of structural damage in the city of Rome. Struct. And Infrastruct. Eng. 10, 1469–1483. https://doi.org/10.1080/15732479.2013.833949

Béjar-Pizarro, M., Notti, D., Mateos, R.M., Ezquerro, P., Centolanza, G., Herrera, G., Bru, G., Sanabria, M., Solari, L., Duro, J., Fernández, J., 2017. Mapping Vulnerable Urban Areas Affected by Slow-Moving Landslides Using Sentinel-1 InSAR Data. Remote Sens. 9, 876. https://doi.org/10.3390/rs9090876

Berardino, P., Fornaro, G., Lanari, R., Sansosti, E., 2002. A new algorithm for surface deformation monitoring based on small baseline differential SAR interferograms. IEEE Trans. on Geosci. and Remote Sens., 40(11), 2375-2383.

Blanco-Sanchez, P., Mallorquí, J. J., Duque, S., Monells, D., 2008. The coherent pixels technique (CPT): An advanced DInSAR technique for nonlinear deformation monitoring. In Earth Sci. and Math. (1167-1193). Birkhäuser Basel.

Bonì, R., Meisina, C., Cigna, F., Herrera, G., Notti, D., Bricker, S., McCormack, H., Tomás, R., Béjar-Pizarro, M., Mulas, J., Ezquerro, P., 2017. Exploitation of Satellite A-DInSAR Time Series for Detection, Characterization and Modelling of Land Subsidence. Geosci. 7, 25. https://doi.org/10.3390/geosciences7020025

Bozzano, F., Cipriani, I., Mazzanti, P., Prestininzi, A., 2011. Displacement patterns of a landslide affected by human activities: Insights from ground-based InSAR monitoring. Nat. Hazards 59, 1377–1396. https://doi.org/10.1007/s11069-011-9840-6

Bozzano, F., Mazzanti, P., Prestininzi, A., Scarascia Mugnozza, G., 2010. Research and development of advanced technologies for landslide hazard analysis in Italy. Landslides 7, 381–385. https://doi.org/10.1007/s10346-010-0208-x

637 Ciampalini, A., Bardi, F., Bianchini, S., Frodella, W., Del Ventisette, C., Moretti, S., Casagli, N., 2014.

638   Analysis of building deformation in landslide area using multisensor PSInSARTM technique. Int. J.

639   of Applied Earth Obs. and Geoinf. 33, 166–180. https://doi.org/10.1016/j.jag.2014.05.011

640 Colesanti, C., Wasowski, J., 2006. Investigating landslides with space-borne Synthetic Aperture Radar

641   (SAR) interferometry. Eng. Geol., 88(3-4), 173-199.

642 Confuorto, P., Di Martire, D., Centolanza, G., Iglesias, R., Mallorqui, J.J., Novellino, A., Plank, S.,

643   Ramondini, M., Thuro, K., Calcaterra, D., 2017. Post-failure evolution analysis of a rainfall-triggered

644   landslide by multi-temporal interferometry SAR approaches integrated with geotechnical analysis.

645   Remote Sens. Environ. 188, 51–72. https://doi.org/10.1016/j.rse.2016.11.002

646 Cruden, D.M.; Varnes, D.J., 1996. Landslides Types and Processes. In Landslides: Investigation and Mit-

647   igation. Transportation Research Board Special Report 247, 36–75.

648 de Capoa, P., D'Errico, M., Di Staso, A., Perrone, V., Perrotta, S., Tiberi, V., 2015. The succession of the

649   Val Marecchia Nappe (Northern Apennines, Italy) in the light of new field and biostratigraphic data.

650   Swiss J. of Geosci. 108, 35–54. https://doi.org/10.1007/s00015-015-0177-0

651 Di Martire, D., Iglesias, R., Monells, D., Centolanza, G., Sica, S., Ramondini, M., Pagano, L., Mallorquí,

652   J.J., Calcaterra, D., 2014. Comparison between Differential SAR interferometry and ground meas-

653   urements data in the displacement monitoring of the earth-dam of Conza della Campania (Italy).

654   Remote Sens. Environ. 148, 58–69. https://doi.org/10.1016/j.rse.2014.03.014

655 Di Martire, D., Ramondini, M., Calcaterra, D., 2015. Integrated monitoring network for the hazard assess-

656   ment of slow-moving landslides at Moio della Civitella (Italy). Rend.On. Soc. Geol. Italiana, 35, 109-

657   112.

658 Di Martire, D., Tessitore, S., Brancato, D., Ciminelli, M. G., Costabile, S., Costantini, M., Graziano, G.

659   V., Minati, F., Ramondini, M., Calcaterra, D. 2016. Landslide detection integrated system (LaDIS)

660   based on in-situ and satellite SAR interferometry measurements. Catena, 137, 406-421.

661 Di Martire, D., Paci, M., Confuorto, P., Costabile, S., Guastaferro, F., Verta, A., Calcaterra, D., 2017. A

662   nation-wide system for landslide mapping and risk management in Italy: The second Not-ordinary

Plan of Environmental Remote Sensing. Int. J. of Applied Earth Obs. and Geoinf. 63, 143–157. https://doi.org/10.1016/j.jag.2017.07.018

Dong, J., Zhang, L., Tang, M., Liao, M., Xu, Q., Gong, J., Ao, M., 2018. Mapping landslide surface displacements with time series SAR interferometry by combining persistent and distributed scatterers: A case study of Jiaju landslide in Danba, China. Remote Sens. Environ. 205, 180–198. https://doi.org/10.1016/j.rse.2017.11.022

Elter, P., Grasso, M., Parotto, M., Vezzani, L., 2003. Structural setting of the Apennine-Maghrebian thrust belt. Episodes 26(3), 205-211.

EWCII, ONU, ISDR, 2003. Europe, Regional consultation in preparation for the second International conference on early warning (EWCII), E. J. Plate, ISDR - International strategy for disaster reduction

Ferretti, A., Prati, C., Rocca, F., 2001. Permanent scatterers in SAR interferometry. IEEE Trans. Geosci. Remote Sens. 39(1), 8-20.

Fiaschi, S., Closson, D., Abou Karaki, N., Pasquali, P., Riccardi, P., Floris, M., 2017. The complex karst dynamics of the Lisan Peninsula revealed by 25 years of DInSAR observations. Dead Sea, Jordan. ISPRS J. Photogramm. Remote Sens. 130, 358–369. https://doi.org/10.1016/j.isprsjprs.2017.06.008

Frodella, W., Ciampalini, A., Bardi, F., Salvatici, T., Di Traglia, F., Basile, G., Casagli, N., 2018. A method for assessing and managing landslide residual hazard in urban areas. Landslides 15, 183–197. https://doi.org/10.1007/s10346-017-0875-y

Giordan, D., Allasia, P., Manconi, A., Baldo, M., Santangelo, M., Cardinali, M., Corazza, A., Albanese, V., Lollino, G., Guzzetti, F., 2013. Morphological and kinematic evolution of a large earthflow: The Montaguto landslide, southern Italy. Geomorphology 187, 61–79. https://doi.org/10.1016/j.geomorph.2012.12.035

Guadagno, F. M., Celico, P. B., Esposito, L., Perriello Zampelli, S., Piscopo, V., Scarascia Mugnozza, G., 1999. The debris flows of 5–6 May 1998 in Campania, southern Italy. Landslide news 12, 5-7.

687 Herrera, G., Tomás, R., Vicente, F., Lopez-Sanchez, J. M., Mallorquí, J. J., Mulas, J., 2010. Mapping
688   ground movements in open pit mining areas using differential SAR interferometry. Int. J. of Rock
689   Mech. and Mining Sci., 47(7), 1114-1125.

690 Herrera, G., Gutiérrez, F., García-Davalillo, J.C., Guerrero, J., Notti, D., Galve, J.P., Fernández-Merodo,
691   J.A., Cooksley, G., 2013. Multi-sensor advanced DInSAR monitoring of very slow landslides: The
692   Tena Valley case study (Central Spanish Pyrenees). Remote Sens. Environ. 128, 31–43.
693   https://doi.org/10.1016/j.rse.2012.09.020

694 Iglesias, Rubén, Mallorqui, J., Monells, D., López-Martínez, C., Fabregas, X., Aguasca, A., Gili, J., Co-
695   rominas, J., 2015. PSI Deformation Map Retrieval by Means of Temporal Sublook Coherence on
696   Reduced Sets of SAR Images. Remote Sens. 7, 530–563. https://doi.org/10.3390/rs70100530

697 Infante, D., Confuorto, P., Di Martire, D., Ramondini, M., Calcaterra, D., 2016. Use of DInSAR Data for
698   Multi-level Vulnerability Assessment of Urban Settings Affected by Slow-moving and Intermittent
699   Landslides. Procedia Eng. 158, 470–475. https://doi.org/10.1016/j.proeng.2016.08.474

700 Infante, D., Di Martire, D., Confuorto, P., Ramondini, M., Calcaterra, D., Tomas, R., Duro, J., Centolanza,
701   G., 2017. Multi-temporal assessment of building damage on a landslide-affected area by interfero-
702   metric data, in: 2017 IEEE 3rd Int. Forum on Res. and Technol. for Soc. and Ind. - Innovation to
703   Shape the Future for Society and Industry (RTSI). pp. 1–6.
704   https://doi.org/10.1109/RTSI.2017.8065907

705 Istituto di Ricerca per la Protezione Idrogeologica (IRPI), del Consiglio Nazionale delle Ricerche (CNR),
706   2018. Periodical report about Landslide and flood hazard to Italian People (In Italian).

707 Lanari, R., Mora, O., Manunta, M., Mallorqui, J.J., Berardino, P., Sansosti, E., 2004. A small-baseline
708   approach for investigating deformations on full-resolution differential SAR interferograms. IEEE
709   Trans. Geosci. Remote Sens. 42, 1377–1386. https://doi.org/10.1109/TGRS.2004.828196

710 Liu, D., Sowter, A., Niemeier, W., 2014. Process-related deformation monitoring by PSI using high reso-
711   lution space-based SAR data: A case study in Düsseldorf, Germany. Nat. Hazards Earth Syst. Sci. 2,
712   4813–4830. https://doi.org/10.5194/nhessd-2-4813-2014

713   Mendelsohn, R., Saher, G., 2011. The global impact of climate change on extreme events. Washington,

714   DC: World Bank.

715   Middelmann, M. H., 2007. Impact of natural disasters. Natural Hazards in Australia: identifying risk anal-

716   ysis requirements. Canberra: Geosci. Australia, 7-29.

717   Milillo, P., Giardina, G., DeJong, M. J., Perissin, D., Milillo, G., 2018. Multi-Temporal InSAR Structural

718   Damage Assessment: The London Crossrail Case Study. Remote Sens., 10(2), 287.

719   Mora, O., Mallorqui, J.J., Broquetas, A., 2003. Linear and nonlinear terrain deformation maps from a

720   reduced set of interferometric SAR images. IEEE Trans. Geosci. Remote Sens. 41, 2243–2253.

721   https://doi.org/10.1109/TGRS.2003.814657

722   Morgenstern, N. R., Price, V. E. 1965. The analysis of the stability of general slip surfaces.

723   Notti, D., Galve, J.P., Mateos, R.M., Monserrat, O., Lamas-Fernández, F., Fernández-Chacón, F., Roldán-

724   García, F.J., Pérez-Peña, J.V., Crosetto, M., Azañón, J.M., 2015. Human-induced coastal landslide

725   reactivation. Monitoring by PSInSAR techniques and urban damage survey (SE Spain). Landslides

726   12, 1007–1014. https://doi.org/10.1007/s10346-015-0612-3

727   Petrucci, O., Gullà, G., 2010. A simplified method for assessing landslide damage indices. Nat. hazards

728   52(3), 539-560.

729   Plank, S., Twele, A., Martinis, S., 2016. Landslide mapping in vegetated areas using change detection

730   based on optical and polarimetric SAR data. Remote Sens. 8(4), 307.

731   Plesi, G., Galli, M., Daniele, G., 2002. The Monti Rognosi Ophioliitc Unit (cfr. Calvana Unit Auct.) pal-

732   aeogeographic position in the External Ligurian Domain, relationships with the tectonic units derived

733   from the Adriatic margin. Boll. Soc. Geol. It. 1, 273–284.

734   Principi, G., Bortolotti, V., Chiari, M., Cortesogno, L., Gaggero, L., Marcucci, M., Saccani, E., Treves,

735   B., 2004. The pre-orogenic volcano-sedimentary covers of the Western Tethys oceanic basin: a re-

736   view. Ofioliti 29, 177-211.

737   Rosen, P.A., Hensley, S., Joughin, I.R., Li, F.K., Madsen, S.N., Rodriguez, E., Goldstein, R.M., 2000.

738   Synthetic aperture radar interferometry, Proc. IEEE 88 (3), 333–382.

739   Sacco, P., Battagliere, M. L., Daraio, M. G., Coletta, A., 2015. The COSMO-SkyMed constellation

740   monitoring of the Italian territory: the Map Italy project. In Proc. of 66th International Astronautical Con-

741   gress (IAC 2015) (pp. 12–16).

742   Salvati, P., Bianchi, C., Rossi, M., Guzzetti F., 2010. Societal landslide and flood risk in Italy, Nat. Haz-

743   ards Earth Syst. Sci. 10, 465-483.

744   Sammarco, O., 2004. A tragic disaster caused by the failure of tailings dams leads to the formation of the

745   Stava 1985 Foundation. Mine Water and the Environ. 23(2), 91-95.

746   Schuster, R. L., Fleming, R. W., 1986. Economic losses and fatalities due to landslides. Bull. Association

747   of Eng. Geol. 23(1), 11-28.

748   Serrano-Juan, A., Pujades, E., Vázquez-Suñè, E., Crosetto, M., Cuevas-González, M., 2017. Leveling vs.

749   InSAR in urban underground construction monitoring: Pros and cons. Case of la sagrera railway sta-

750   tion (Barcelona, Spain). Eng. Geol. 218, 1-11.

751   Sousa, J. J., Bastos, L., 2013. Multi-temporal SAR interferometry reveals acceleration of bridge sinking

752   before collapse. Nat. Hazards Earth Syst. Sci. 13(3), 659.

753   Strozzi, T., Teatini, P., Tosi, L., 2009. TerraSAR-X reveals the impact of the mobile barrier works on

754   Venice coastland stability. Remote Sens. Environ. 113(12), 2682-2688.

755   Strozzi, T., Delaloye, R., Poffet, D., Hansmann, J., Loew, S., 2011. Surface subsidence and uplift above a

756   headrace tunnel in metamorphic basement rocks of the Swiss Alps as detected by satellite SAR inter-

757   ferometry. Remote Sens. Environ. 115, 1353–1360.

758   Tarquini S., I. Isola, M. Favalli, F. Mazzarini, M. Bisson, M.T. Pareschi, E. Boschi, 2007. TINITALY/01:

759   a new Triangular Irregular Network of Italy, Ann.of Geoph. 50, 407-425.

760   Tarquini S., Vinci S., Favalli M., Doumaz F., Fornaciai A., Nannipieri L., 2012. Release of a 10-m-reso-

761   lution DEM for the Italian territory: Comparison with global-coverage DEMs and anaglyph-mode

762   exploration via the web, Comp. & Geosci. 38, 168-170. doi: doi:10.1016/j.cageo.2011.04.018

763   Tessitore, S., Fernández-Merodo, J. A., Herrera, G., Tomás, R., Ramondini, M., Sanabria, M., Calcaterra,

764   D., 2016. Comparison of water-level, extensometric, DInSAR and simulation data for quantification

765   of subsidence in Murcia City (SE Spain). Hydrogeol. J 24(3), 727.

766   Tessitore, S., Di Martire, D., Calcaterra, D., Infante, D., Ramondini, M., Russo, G., 2017. Multitemporal

767   synthetic aperture radar for bridges monitoring. In Remote Sensing Technologies and Applications

768   in Urban Environments II (Vol. 10431, p. 104310C). International Society for Optics and Photonics.

769   Tofani, V., Raspini, F., Catani, F., Casagli, N., 2013. Persistent Scatterer Interferometry (PSI) technique

770   for landslide characterization and monitoring. Remote Sens. 5(3), 1045-1065.

771   Tofani, V., Del Ventisette, C., Moretti, S., Casagli, N., 2014. Integration of Remote Sensing Techniques

772   for Intensity Zonation within a Landslide Area: A Case Study in the Northern Apennines, Italy, Re-

773   mote Sens. 6, 907-924.

774   Tuscany Coast Authority, Hydro-geomorphological Setting Plan, November 2012, http://www.re-

775   gione.toscana.it/-/piano-di-bacino-bacino-regionale-toscana-costa- (in Italian)

776   United Nations, 2010. Natural hazards, unnatural disasters: the economics of effective prevention. The

777   World Bank.

778   Vranken, L., Van Turnhout, P., Van Den Eeckhaut, M., Vandekerckhove, L., Poesen, J. 2013. Economic

779   valuation of landslide damage in hilly regions: A case study from Flanders, Belgium. Sci. Total En-

780   viron. 447, 323-336.

781   Wasowski, J., Bovenga, F., 2014. Investigating landslides and unstable slopes with satellite Multi Tem-

782   poral Interferometry: Current issues and future perspectives, Eng. Geol. 174, 103–138.

783   www.geostru.com/EN/Slopestability-analysis.aspx accessed on 20 June 2018

784   www.geostru.eu/shop/geotechnical-software/gfas-geotechnical-f-e-m-analysis-system/ accessed on 20

785   June 2018

786   www.sir.toscana.it/pluviometria-pub accessed on 10 December 2018

787